TECHNISCHE MECHANIK, Band 26, Heft 1, (2006), 33– 43
Manuskripteingang: 31. Januar 2006

Wrinkling Analysis of Thermo–Elastic Membranes

Jörg Hornig, Heinrich Schoop, Uwe Herbrich

In order to analyze the state of stress in extremely thin membranes, the wrinkling phenomenon has to be taken into account. This paper concerns numerical analysis of thermo–elastic membrane wrinkling. Based on an algorithm for hyper-elastic membranes, thermo–elastic effects will be included in the wrinkling theory. Formulations of the thermo–elastic wrinkling algorithm for small strains and for large strains are given. Winkling effects of thermally loaded rubber membranes with large strains have been analyzed. Heat conduction is neglected in these considerations. Results of finite element analysis of membrane structures are presented.

1 Introduction

Membranes are very suitable to carry tensile loads but they fail partially or completely if compressive in-plane loads occur. Since ideal membranes do not possess any flexural stiffness, they can not carry compressive in–plane loads. In this case membranes wrinkle and lose partially or completely their capability to carry loads. It can be essential to take wrinkling effects into account.

Wrinkling of membranes was investigated by many scientists in the past. Some recent works on wrinkling analysis were published by Roddeman (1987), Taenzer (1997), Seokwoo and Seyoung (1997), Lu et al. (2001), Ziegler et al. (2000), Wiedemann (2002) and Raible (2003). Some membranes, like space structures, are exposed to large changes in temperature. The effect of heating or cooling on the wrinkling behavior will influence the mechanical behavior of membranes. The influence of temperature effects on membrane wrinkling was firstly studied by Chiu et al. (1994).

In the present paper a wrinkling theory for thermo–elastic membranes is described, based on a reference–related formulation (see Schoop et al. (2002)). For many thermo–elastic problems the small strain assumption is justified. The extension of the existing wrinkling theory based on the small strain assumption is simple. The wrinkling algorithm for thermo–elastic membranes with large strains is obtained by a modification of the wrinkling algorithm for elasto–plastic membranes, published in Hornig and Schoop (2005). Especially the behavior of thermo–elastic rubber membranes will be considered here. A description of thermo–elasticity of rubber can be found in, e.g., Holzapfel and Simo (1996), Miehe (1995) and Holzapfel (2004).

In general membranes should be considered in a nonlinear setting, since they may undergo large rotations and, occasionally, large strains. Complex nonlinear problems in structural mechanics are often solved by means of the finite element method. In order to balance the internal and the outer nodal forces, it is necessary to determine the state of stress (or membrane forces) at the integration points of the finite elements. However, the state of membrane forces can be influenced by membrane wrinkling. The wrinkling can be taken into account by means of a wrinkling algorithm. The algorithm ensures that finite membrane elements are free of compressive principal membrane forces and provides correct membrane stiffnesses depending on the wrinkling state.

2 Wrinkling Theory for Hyper-Elastic Membranes without Thermal Effects

Membrane wrinkling is an instability phenomenon of very thin–walled surface structures under compression and shear loads (i.e. buckling in terms of the theory of shells). Unless the FE–mesh is extremely fine, the finite shell elements are not able to represent a short wave wrinkling pattern. In order to take such deformations into account for the ideal membrane model, a kinematic correction will be added to the FE interpolated deformation state. The material behavior of the membrane itself remains unchanged. By means of this kinematic correction, the load transition behavior of the membrane structure can be analyzed. The detailed wave pattern of the wrinkled membrane remains undetermined. Depending on the applied loads, a membrane can achieve one of the following three states

1. taut state: only tension forces in the membrane, full capability to carry loads
2. slack state: no membrane forces in the membrane, no capability to carry loads
3. regularly wrinkled state: load transition due to an uniaxial state of membrane force

If only a few integration points have a slack state, the membrane may have stable load carrying characteristics and the FE calculation will converge, otherwise it may fail. In order to distinguish these three states for given deformations of the finite element, a wrinkling criterion has to be established.

Wrinkling criterion. Several wrinkling criteria have been developed in the past, either based on the state of membrane force (see, e.g. Otto and Trostel (1962)) or on the state of strain (see, e.g. Miller et al. (1985)). Roddeman (1987) introduced a mixed wrinkling criterion, using both, membrane forces and strains to distinguish the three wrinkling states. Here a mixed wrinkling criterion is applied. Knowing the (FE–interpolated) planar Green strains $\mathbf{D}$, and the corresponding uncorrected 2nd Piola–Kirchhoff membrane force tensor $\mathbf{S}(\mathbf{D})$ the wrinkling state can be identified in the following way

- taut state: $S_I > S_{II} > 0$
- slack state: $D_{II} < D_I < 0$
- homogeneous wrinkled state: otherwise

D_I, D_{II}, S_I and S_{II} are the principal values of strains and membrane forces, respectively, while the first principal value is the larger one.

So far the membrane is stretched in at least one direction and a tension membrane forces will arise, even in the case if the uncorrected (i.e. unwrinkled) membrane forces are compressive (due to Poisson's effect). Under such a loading, the membrane will wrinkle and the uncorrected biaxial state of stress will switch to a uniaxial state with tension.

If for given FE-interpolated strains a certain wrinkling state is detected, the analysis proceeds this way: In case of a taut membrane, the analysis is conducted in a common way. If the membrane is slack, membrane forces and stiffnesses will be set to zero. For a regularly wrinkled membrane additional considerations have to be made, in order to determine the state of membrane force. The kinematics and the uniaxial state of membrane forces of regularly wrinkled membranes are considered in more detail.

Membrane forces. For membranes the plane state of stress is assumed, i.e. only the planar stress components $T_{\alpha\beta}$ may differ from zero. $T_{\alpha\beta}$ denotes the planar 2nd Piola–Kirchhoff stresses. Greek indices take the values 1 or 2, thus $\alpha, \beta = 1, 2$ (unless mentioned otherwise, bold characters denote planar quantities like membrane strains and membrane forces). The components of the 3D–stress tensor T_{ij} (with $i, j = 1, 2, 3$) follow from the derivative of the strain energy function $\Psi\,(C_{ij})$ with respect to the Cauchy–Green strains C_{ij}

$$T_{ij} = 2\,\frac{\partial \Psi}{\partial C_{ij}} \tag{1}$$

C_{13}, C_{23}, T_{13} and T_{23} are assumed to be zero. The thickness strain C_{33} is determined by the plane stress requirement $T_{33} = 0$. Planar stresses and the 2nd Piola–Kirchhoff membrane forces are related by

$$S_{\alpha\beta} = h\,T_{\alpha\beta} \tag{2}$$

h is the membrane thickness in the reference configuration. In this paper the St. Venant material and the Mooney–Rivlin material will be considered in more details, i.e. for St. Venant material

$$T_{\alpha\beta} = 2G\left(D_{\alpha\beta} + \frac{\nu}{1-\nu}\,(D_{11} + D_{22})\,\delta_{\alpha\beta}\right) \tag{3}$$

and for the Mooney–Rivlin material

$$T_I = \left(1 - \frac{1}{{\lambda_1}^4\,{\lambda_2}^2}\right)\left(\mu_1 - \mu_2\,{\lambda_2}^2\right) \qquad T_{II} = \left(1 - \frac{1}{{\lambda_1}^2\,{\lambda_2}^4}\right)\left(\mu_1 - \mu_2\,{\lambda_1}^2\right) \tag{4}$$

Equations 4 describe the principal 2nd Piola–Kirchhoff stresses of an isochoric rubber–like material in dependency on the pricipal stretches λ_1 and λ_2 (see Holzapfel (2004) for details). G is the shear modulus, ν the Poissons ratio and μ_1 and μ_2 are rubber material data with $2G = \mu_1 - \mu_2$. The plane stress condition is satisfied in the equations 3 and 4.

Figure 1 shows the regions of the three wrinkling states in the space of principal strains D_I, D_{II} or principal stretches λ_1, λ_2, respectively. The left picture is for a St.Venant material in the D_I–D_{II} space, the right picture is for a Mooney–Rivlin material in the λ_1–λ_2 space. The grey marked areas are the regions in the strain space where regular wrinkling takes place. By definition $\lambda_1 > \lambda_2$ holds.

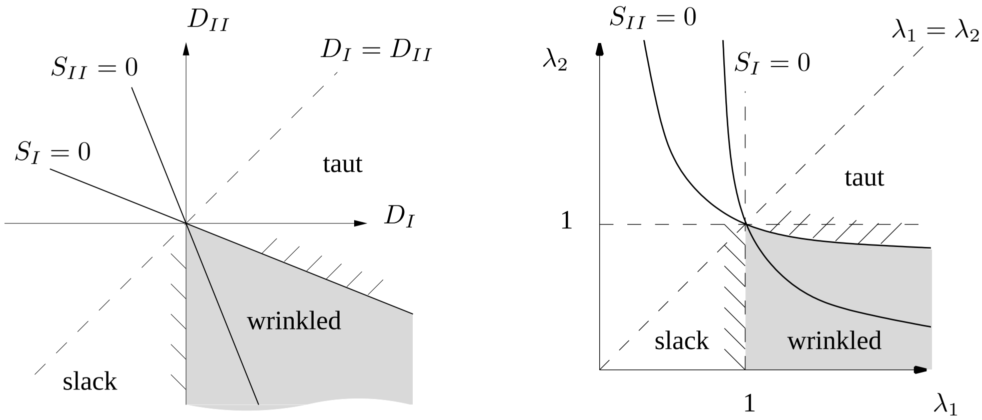

Figure 1: Membrane states of isotropic membranes – in principal Green strains for a St. Venant material (left) and in principal stretch for a Mooney-Rivlin material (right)

Beside the wrinkling phenomenon for rubber membranes, additional instabilities in biaxial tension are known (see Kearsley (1986) and Müller and Strehlow (2004)). This instability will not influence the wrinkling phenomenon since it occurs for symmetric tension only, i.e for $S_I = S_{II} > 0$.

Wrinkling kinematics. Deformations caused by regular wrinkling can be taken into account by adding a correction term to the FE–interpolated deformation gradient[1] $\mathbf{F}$

$$\mathbf{F}' = (\mathbf{E}_3 + \beta_R \mathbf{n} \circ \mathbf{n}) \cdot \mathbf{F}, \tag{5}$$

where $\mathbf{n}$ describes the wrinkling direction as depicted in Figure 2. $\mathbf{E}_3$ is the 3D–unit tensor, β_R is Roddeman's wrinkling parameter (with $\beta_R > 0$). A prime $(\quad)'$ denotes corrected quantities. Since both deformation gradients $\mathbf{F}$ and $\mathbf{F}'$ describe a map from the reference plane into the space, they can be written as 3×2–matrices. By means of the wrinkling kinematics the true length of the wrinkled membrane is represented.

As shown by Schoop et al. (2002), a similar representation can be found for the Green strain tensor and the right Cauchy–Green strain tensor

$$\mathbf{D}' = \mathbf{D} + \beta \mathbf{N} \circ \mathbf{N} \qquad \text{and} \qquad \mathbf{C}' = \mathbf{C} + 2\beta \mathbf{N} \circ \mathbf{N} \tag{6}$$

with the FE–interpolated strain tensors $\mathbf{D}$, $\mathbf{C}$, the reference related wrinkling parameter β and the vector $\mathbf{N}$, placed in the $\mathbf{e}_1$– $\mathbf{e}_2$ reference plane, representing a wrinkling direction: $\mathbf{N} = \cos\alpha\,\mathbf{e}_1 + \sin\alpha\,\mathbf{e}_2$. The same as Roddeman's parameter β_R, the wrinkling parameter β is always positive.

[1] The tensor product of two vectors $x_i \mathbf{g}^i \circ y_j \mathbf{g}^j$ is defined by $\mathbf{x} \circ \mathbf{y} = \; x_i y_j \mathbf{g}^i \circ \mathbf{g}^j$

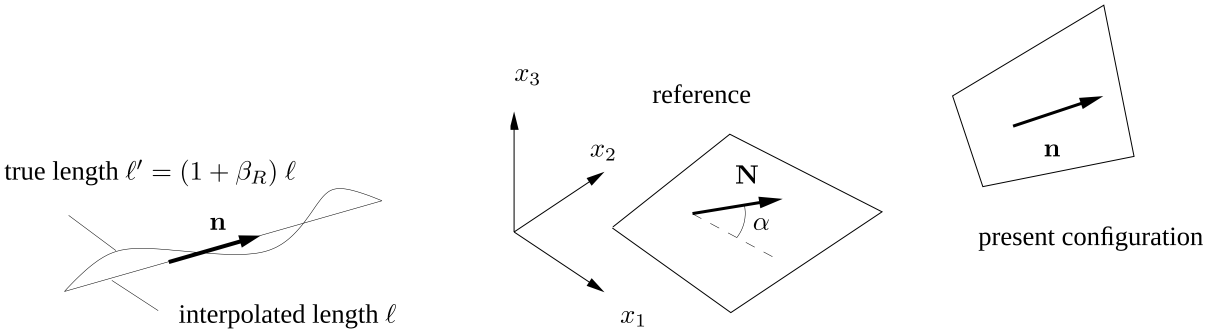

Figure 2: Measures of length and wrinkling direction of a wrinkled membrane

Wrinkling condition. In a regularly wrinkled membrane a uniaxial state of membrane forces exists. For the wrinkling conditions, Schoop et al. (2002) gave the following representation in terms of the 2nd Piola–Kirchhoff membrane force tensor $\mathbf{S}$

$$0 = \mathbf{N}\cdot\mathbf{S}\,(\mathbf{D}')\cdot\mathbf{N} = f_1(\alpha,\beta) \tag{7}$$
$$0 = \mathbf{N}\cdot\mathbf{S}\,(\mathbf{D}')\cdot\mathbf{N}_\perp = f_2(\alpha,\beta) \tag{8}$$

Vector $\mathbf{N}_\perp = -\sin\alpha\,\mathbf{e}_1 + \cos\alpha\,\mathbf{e}_2$ is located in the reference plane, perpendicular to $\mathbf{N}$.

The equations 7 and 8 are a set of equations for the two unknowns α and β. These nonlinear equations can be solved by Newton's method. From the wrinkling condition, the wrinkling direction α and the wrinkling parameter β can be calculated and the state of membrane forces will be determined. This procedure is carried out at every integration point of the finite elements. In Schoop et al. (2002) a consistent linearization is given, which yields the correct stiffness of the wrinkled membrane.

3 Thermo–Elastic Wrinkling for Small Strains

In this paragraph the wrinkling of membranes which are exposed to a change of temperature $\vartheta = \theta - \theta_0$ is under investigation. θ_0 is the reference temperature. Strains are assumed to be small. Hence an additive split of Green's strain tensor into elastic strains $\mathbf{D}_e$ and thermal strains $\mathbf{D}_\theta$ is admissible

$$\mathbf{D} = \mathbf{D}_\theta + \mathbf{D}_e \qquad \text{with} \qquad \mathbf{D}_\theta = \vartheta\,\boldsymbol{\alpha}_\theta \tag{9}$$

$\boldsymbol{\alpha}_\theta$ are linear coefficients of thermal expansion for a thermal anisotropic material. For an isotropic material $\boldsymbol{\alpha}_\theta = \alpha_\theta\,\mathbf{E}$ holds. The 2nd Piola–Kirchhoff membrane forces follow from thermo–elastic constitutive equations

$$\mathbf{S}(\mathbf{D},\theta) = \mathbb{C}\cdot\cdot(\mathbf{D} - \mathbf{D}_\theta) \tag{10}$$

with the 4th order elasticity tensor $\mathbb{C}$.

Wrinkling criterion. In order to take the temperature effects on the wrinkling states into account, the wrinkling criterion presented above has to be modified. Hereby a slack state is assumed if the principal values of the elastic strains $\mathbf{D}_e = \mathbf{D} - \mathbf{D}_\theta$ are solely compressive.

- taut state: $S_I > S_{II} > 0$
- slack state: $D_{e,II} < D_{e,I} < 0$
- regularly wrinkled state: otherwise

Using the corrected membrane forces $\mathbf{S}(\mathbf{D}',\theta) = \mathbb{C}\cdot\cdot(\mathbf{D}' - \mathbf{D}_\theta)$ in the wrinkling conditions 7 and 8 gives a system of equations for the wrinkling direction α and the wrinkling parameter β.

3.1 Numerical Example – Solar Sail

Solar sails are currently investigated as an alternative propellant in space for satellites. The solar sail is subjected to the sun pressure, which provides a small but permanent driving force. Since the sun pressure depends on the light angle of incidence, the deflection of the membrane can influence the performance of the solar sail. The structure of the satellite is subjected to changing temperatures. The effect of the temperature on the sail deflection is investigated next. Here, the solar sail is modeled as a membrane with fixed corners and a fixed center. No further structural elements are taken into account. In the reference configuration the membrane is plane and square. Geometry and conditions of bearing are shown in Figure 3. The solar sail is made of a polyamide–foil. This foil is characterized by an isotropic material behavior. Thermal strains are described by equation 9. The membrane is loaded by the sun pressure $p = 0.92 \cdot 10^{-5}\mathrm{N/mm}^2$ and a temperature difference $\vartheta = \pm 100$ K. In the computations the sun pressure is treated as a fluid pressure load. Data of the solar sail are:

- width $a = 10000$ mm
- thickness of membrane $h = 7.6 \cdot 10^{-3}$ mm
- Young's modulus $E = 2000 \frac{\mathrm{N}}{\mathrm{mm}^2}$
- Poisson's ratio $\nu = 0.3$
- coefficient of thermal expansion $\alpha_\theta = 8.0 \cdot 10^{-5} \frac{1}{\mathrm{K}}$
- sun pressure $p = 0.92 \cdot 10^{-5} \frac{\mathrm{N}}{\mathrm{mm}^2}$
- temperature difference $\vartheta = \pm 100$ K

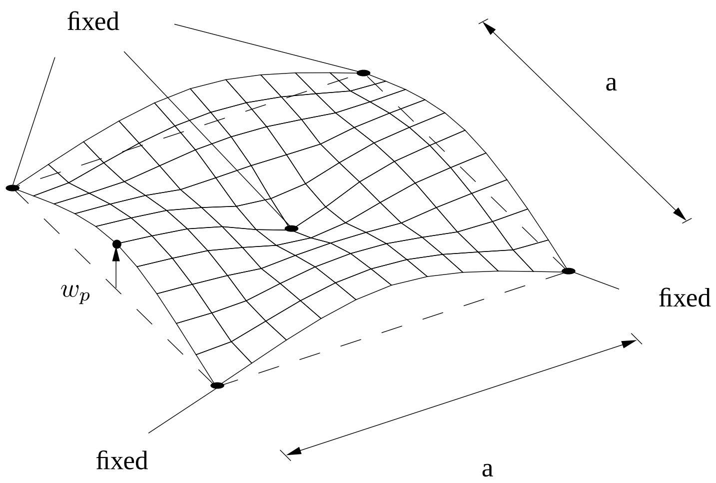

Figure 3: Geometry and bearing of the solar sail

Figures 4 to 6 show state of wrinkling for the solar sail loaded with sun pressure and temperature differences of $\vartheta = 0$ K and $\vartheta = \pm 100$ K, respectively. Wrinkles at integration points are depicted by lines along the wrinkling direction (i.e. direction of the vanishing principle membrane force). A rhombus marks integration points with a slack membrane.

In all considered cases wrinkles appear in the surrounding of the membrane diagonals. For $\vartheta = -100$ K the wrinkling is in general reduced. In this case the center of the membrane is taut, while for the heated membrane ($\vartheta = +100$ K) wrinkles appear at the center. The midpoint deflection w_P of an edge (see Figure 3) is under consideration. The deflection grows with increasing temperature. For the three considered temperatures the following values were obtained by the numerical simulations

- $w_P = 733.9$ mm at $\vartheta = -100$ K
- $w_P = 890.3$ mm at $\vartheta = 0$ K

- $w_P = 1050.9$ mm at $\vartheta = 100$ K

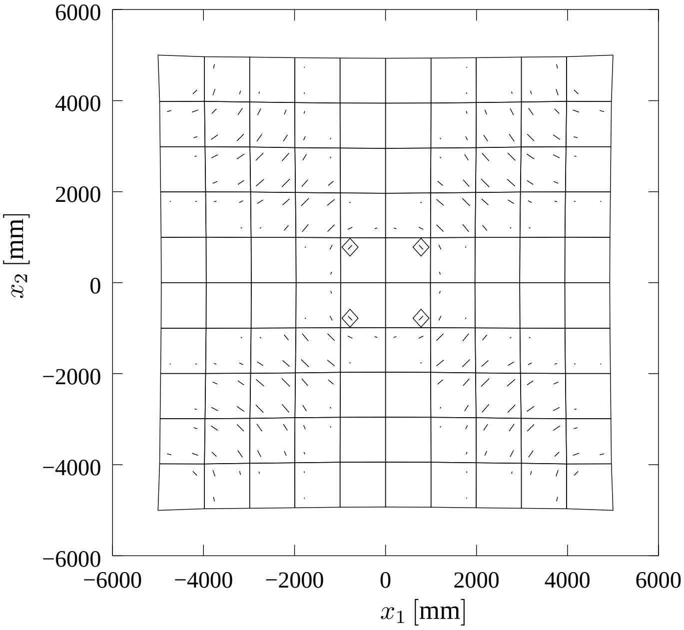

Figure 4: Top view of the solar sail under thermal and sun pressure load, state of wrinkling at $\vartheta = -100$ K

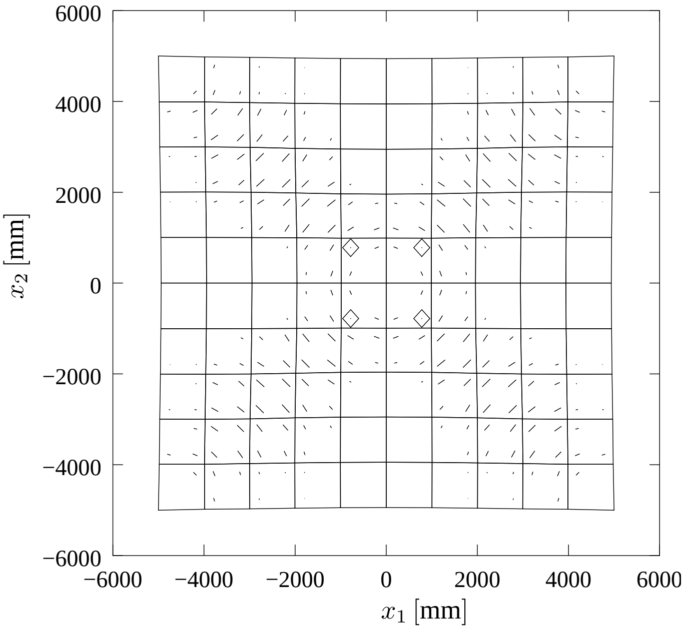

Figure 5: Top view of the solar sail under thermal and sun pressure load, state of wrinkling at $\vartheta = 0$ K

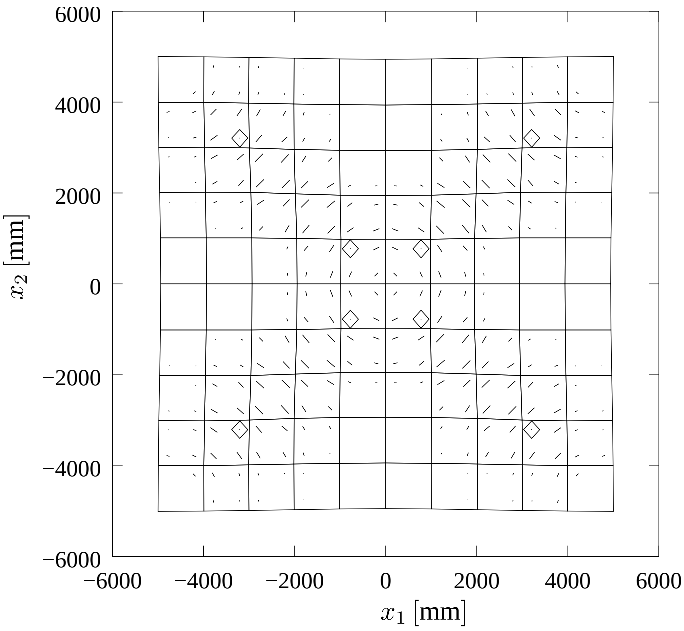

Figure 6: Top view of the solar sail under thermal and sun pressure load, state of wrinkling at $\vartheta = +100$ K

4 Thermo–Elasticity for Large Strains

Thermo–elastic deformations. The concept of a multiplicative decomposition of $\mathbf{F}$ will be applied. The deformation gradient of the membrane is split into an purely elastic deformation $\mathbf{F}_e$ and a purely thermal deformation $\hat{\mathbf{F}}(\theta)$ depending on the temperature θ

$$\mathbf{F} = \mathbf{F}_e \cdot \hat{\mathbf{F}} \tag{11}$$

The elastic and thermal Cauchy–Green strain measures

$$\hat{\mathbf{C}} = \hat{\mathbf{F}}^T \cdot \hat{\mathbf{F}} \qquad \mathbf{C}_e = \mathbf{F}_e^T \cdot \mathbf{F}_e \quad \text{with } \mathbf{C} = \hat{\mathbf{F}}^T \cdot \mathbf{C}_e \cdot \hat{\mathbf{F}} \tag{12}$$

are introduced. $\mathbf{C}$, $\hat{\mathbf{C}}$ and $\mathbf{C}_e$ are planar strain measures of the membrane. A multiplicative decomposition of the corrected deformation gradient $\mathbf{F}'$ can be done in the same way. The thermal strains will be specified in Section 4.1 for a rubber–like material.

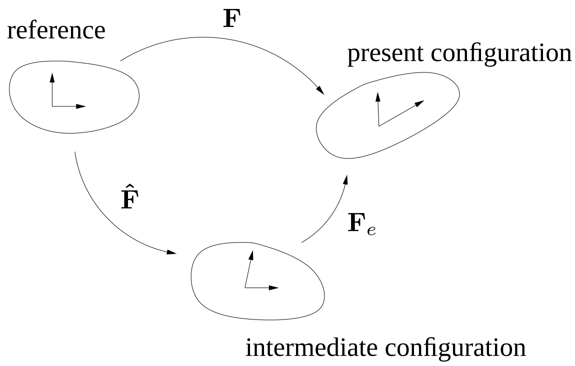

Figure 7: Thermo–elastic deformation of a membrane

The membrane forces. In case of a thermo–elastic material the 2nd Piola–Kirchhoff stresses are the derivative of the Helmholtz free energy $\Psi(C_{ij}, \theta)$ with respect to the right Cauchy–Green strains (see Holzapfel (2004)). The membrane forces read

$$S_{\alpha\beta}(\mathbf{C}, \theta) = h\, T_{\alpha\beta} \qquad \text{with} \qquad T_{ij} = 2\, \frac{\partial \Psi}{\partial C_{ij}} \tag{13}$$

In a membrane the thickness strain C_{33} is determined by the plane stress requirement $T_{33} = 0$.

Wrinkling criterion. The same concept as already presented for the small strain case can be applied here, in particular, a slack membrane is assumed if elastic strains are completely compressive.

- taut state: $S_I > S_{II} > 0$
- slack state: $C_{e,II} < C_{e,I} < 1$
- regularly wrinkled state: otherwise

Thus, in order to detect a slack state the principal values of $\mathbf{C}_e$ have to be evaluated. According to Tietze (1986), the 1st and 2nd invariants of $\mathbf{C}_e$ equal those of $(\hat{\mathbf{C}}^{-1} \cdot \mathbf{C})$:

$$I_1 = \mathbf{C}_e \cdot\cdot \mathbf{E} = (\hat{\mathbf{C}}^{-1} \cdot \mathbf{C}) \cdot\cdot \mathbf{E} \tag{14}$$

$$I_2 = \mathbf{C}_e \cdot\cdot \mathbf{C}_e = (\hat{\mathbf{C}}^{-1} \cdot \mathbf{C}) \cdot\cdot (\hat{\mathbf{C}}^{-1} \cdot \mathbf{C}) \tag{15}$$

If the purely thermal strains $\hat{\mathbf{C}}$ and the total strain $\mathbf{C}$ are known, the principal values of $\mathbf{C}_e$ can be determined. Using the invariants I_1 and I_2, obtained by equation 14 and 15, the midpoint M and the radius r of $\mathbf{C}_e$–Mohr's circle are given by

$$M = \frac{1}{2}\, I_1 \qquad r = \frac{1}{2}\sqrt{2I_2 - I_1^2} \tag{16}$$

Then, the principal values of $\mathbf{C}_e$ are

$$C_{e,I} = M + r \qquad C_{e,II} = M - r \tag{17}$$

Wrinkling condition. In a regularly wrinkled membrane the uniaxial state of membrane forces is required. Since the thermal effects influence the membrane forces, the wrinkling conditions are

$$0 = \mathbf{N} \cdot \mathbf{S}(\mathbf{C}', \theta) \cdot \mathbf{N} \tag{18}$$

$$0 = \mathbf{N} \cdot \mathbf{S}(\mathbf{C}', \theta) \cdot \mathbf{N}_\perp \tag{19}$$

with $\mathbf{C}'$ according equation 6. From these nonlinear equations the wrinkling direction α and wrinkling parameter β can be determined by means of Newton's method.

4.1 Constitutive Equations for a Rubber–like Material

As an example for thermo–elastic wrinkling rubber like membranes are considered. The description of the material behavior is based on the extended Ogden model for slightly compressive rubber (see Holzapfel (2004)). The relation of a purely thermal deformation $\hat{F}_{ij}$ caused by a change of temperature $\vartheta = \theta - \theta_0$, is

$$\hat{F}_{ij} = F(\theta)\, \delta_{ij} \qquad \text{with} \qquad F(\theta) = e^{\alpha_\theta\ (\theta - \theta_0)} \tag{20}$$

with the thermal expansion coefficient α_θ, here assumed to be constant.

The notation for the principal stretches used in Holzapfel (2004) will be applied here: λ_i for total principal stretches, $\bar{\lambda}_i = J^{-\frac{1}{3}}\ \lambda_i$ for isochoric principal stretches with $i, j = 1, 2, 3$ and $J = \det(F_{ij})$. Consequently, the principal values of the planar tensor $\mathbf{C}$ are λ_1^2 and λ_2^2.

The Helmholtz free energy Ψ is split into a volumetric and an isochoric part:

$$\Psi(\lambda_1, \lambda_2, \lambda_3, \theta) = \Psi_{vol}(J, \theta) + \Psi_{iso}(\bar{\lambda}_1, \bar{\lambda}_2, \bar{\lambda}_3, \theta) \tag{21}$$

Volumetric and isochoric stress contributions are

$$T_{ij}^{vol} = 2\,\frac{\partial \Psi_{vol}}{\partial C_{ij}} = J\, p\, {C_{ij}}^{-1} \quad \text{and} \quad T_{ij}^{iso} = 2\,\frac{\partial \Psi_{iso}}{\partial C_{ij}} \hat{=} \sum_{a=1}^{3} T_{iso\ a}\, \bar{\mathbf{N}}_a \circ \bar{\mathbf{N}}_a \tag{22}$$

$\bar{\mathbf{N}}_a$ denote the principal directions of stretch, identical with the principal directions of $\mathbf{C}$. For slightly compressible rubber the hydrostatic pressure p follows from the constitutive equation.

$$p = \frac{\partial \Psi_{vol}}{\partial J} = \kappa_0 \frac{\theta}{\theta_0} \frac{dG(J)}{dJ} - \frac{de_0(J)}{dJ} \frac{\vartheta}{\theta_0} \qquad \text{with} \tag{23}$$

$$G(J) = \frac{1}{4} \left(J^2 - 1 - 2 \ln J \right) \qquad \text{and} \tag{24}$$

$$e_0(J) = 3 \, \alpha_\theta \, \kappa_0 \, \theta_0 \, (J - 1) \tag{25}$$

κ_0 is the bulk modulus at θ_0. The relation for the isochoric principal stresses $T_{iso\ a}$ is

$$T_{iso\ a} = \frac{1}{\lambda_a} \frac{\partial \Psi_{iso}}{\partial \lambda_a} = \frac{1}{\lambda_a^2} \sum_{p=1}^{N} \mu_p(\theta) \left(\bar{\lambda}_a^{\alpha_p} - \frac{1}{3} \sum_{b=1}^{3} \bar{\lambda}_b^{\alpha_p} \right) \tag{26}$$

$\mu_p(\theta) = \mu_p(\theta_0) \frac{\theta}{\theta_0}$ are shear moduli and α_p are dimensionless constants with $2G(\theta_0) = \sum_{p=1}^{N} \mu_p(\theta_0)\alpha_p$. In this paper the number of constants is set to $N = 2$ with $\alpha_1 = 2$ and $\alpha_2 = -2$, which corresponds to the Mooney–Rivlin material.

Heat production due to the deformation of the rubber and heat conduction were neglected in these considerations. Hence the isothermal stiffness of the material has to be used in the Newton iteration of the wrinkling algorithm. The plane stress requirement $T_{33} = 0$ is satisfied by means of an iteration procedure which is incorporated into the wrinkling algorithm (see Hornig (2004) for details).

4.2 Numerical Example – Twist of a Cylindric Membrane

In this paragraph a cylindrical rubber membrane under torsional and thermal load is analyzed. Both edges of the cylinder are attached to rigid discs as depicted in Figure 8. The height of the cylinder remains constant during the rotation of the lower disc. A change of temperature $\vartheta = \pm 20$ K is applied and the temperature is fixed at this level during the deformation of the membrane. The membrane was modeled by an 8×12 mesh of bilinear elements. Geometrical data and material properties are:

- radius $R = 100$ mm
- height $H = 300$ mm
- thickness of membrane $h = 0.1$ mm
- reference temperature $\theta_0 = 273.15$ K
- parameters of the Mooney-Rivlin material
  $\mu_1 = 0.3696$ N/mm^2, $\mu_2 = -0.0528$ N/mm^2
  $\alpha_1 = 2$, $\alpha_2 = -2$
- bulk modulus $\kappa_0 = 4.0832$ N/mm^2 which corresponds to a Poisson's ratio $\nu = 0.45$
- coefficient of thermal expansion $\alpha_\theta = 22.333 \cdot 10^{-5} \frac{1}{\text{K}}$

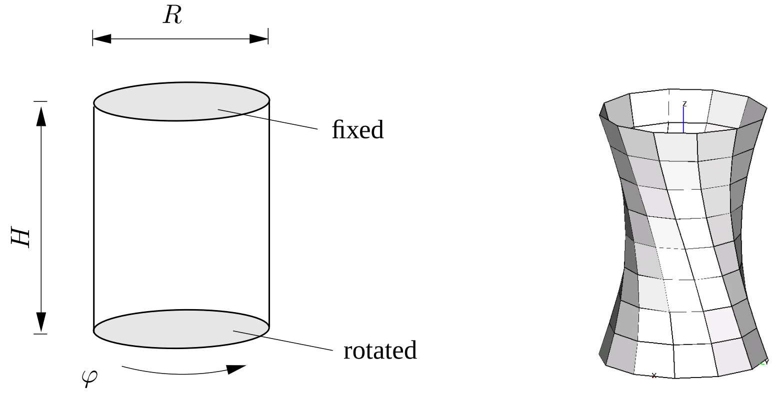

Figure 8: Geometry of the cylinder and deformed shape of the cooled membrane at twist angle $\varphi = 45^o$

Figure 9 shows the resulting torsional moment M_T due to an applied rotation of the lower cylinder edge. M_T is plotted for the membrane at reference temperature $\theta_0 = 273.15$ K and for $\vartheta = \pm 20$ K. In addition the FE solution without wrinkling algorithm is shown by the dashed line. For the depicted range it fits well to the analytical solution of a twisted cylinder. Assuming a homogeneous state of deformation with $D_{11} = 0$, $D_{12} = \frac{1}{2}\frac{\varphi}{L}R$ and $D_{22} = \frac{1}{2}\frac{\varphi^2}{L^2}R^2$ the torsional moment is $M_T = 2G\pi R^3 h\frac{\varphi}{L}$.

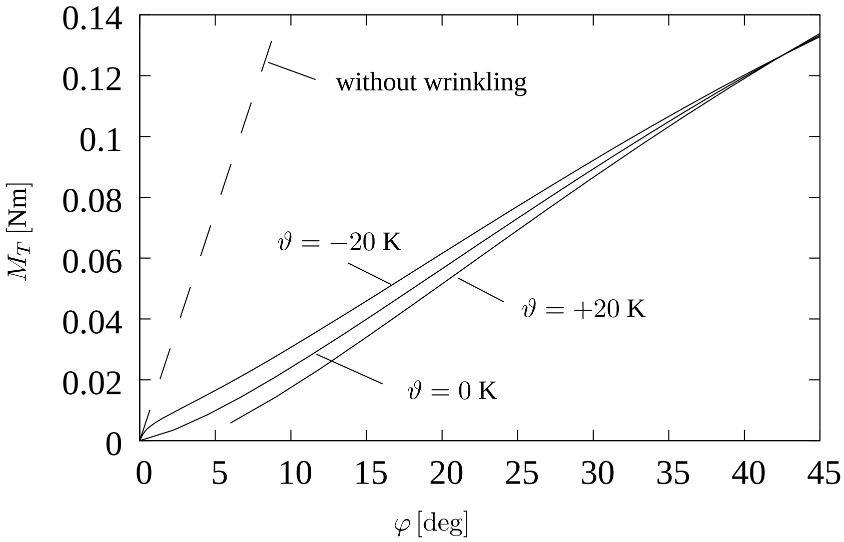

Figure 9: Twist of cylindrical membrane

From the graphs in Figure 9 the influence of the wrinkling phenomenon is clearly visible. Without the wrinkling algorithm M_T is overestimated.

In the range of $\varphi = 0^o$ to 42^o the torsional moment is the higher the lower the temperature is. In the case of the cooled membrane the curve starts relatively steep, with a slope close to that of the curve without wrinkling influence. No convergence of the FE algorithm could be achieved for small angles and $\vartheta = +20$ K, because of zero stiffness of the slack membrane. At $\varphi \approx 42^o$ the M_T–curves for all three temperature cross each other and the M_T of the heated membrane commences to exceed the moment of the cooled membrane. This is a consequence of temperature–dependency of shear moduli $\mu_p(\theta) = \mu_p(\theta_0)\frac{\theta}{\theta_0}$.

5 Summary

In this paper an algorithm for thermal wrinkling of membranes is presented. Beginning from the modified, reference related Roddeman theory, special formulations of wrinkling criteria and wrinkling conditions are given for thermo–elastic membranes. The wrinkling algorithms for thermo–elastic wrinkling analysis is easy to implement into existing FE-programs. The wrinkling analysis takes place at the integration points of finite membrane elements and does not require changes of the structure of the FE–program. Since the basic idea is to apply a correction to the kinematics, different constitutive equations can be applied. Numerical examples show the capability of the presented method to treat wrinkling and thermo–elastic effects.

References

Chiu, H. C.; Benson, R. C.; Fiscella, M. D.; Burns, S. J.: Mechanical and thermal wrinkling of polymer membranes. *Journal of Applied Mechanics*, 61, (1994), 67 – 70.

Holzapfel, G. A.: *Nonlinear Solid Mechanics*. Wiley, Chichester (2004).

Holzapfel, G. A.; Simo, J. C.: Entropy elasticity of isotropic rubber–like solids at finite strains. *Computer Methods in Applied Mechanics and Engineering*, 132, (1996), 17 – 44.

Hornig, J.: *Analyse der Faltenbildung in Membranen aus unterschiedlichen Materialien*. Institut für Mechanik, TU Berlin (2004).

Hornig, J.; Schoop, H.: Wrinkling analysis of membranes with elastic–plastic material behavior. *Computational Mechanics*, 35, (2005), 153–160.

Kearsley, E. A.: Asymmetric stretching of a symmetrically loaded elastic sheet. *Int. J. Solids Structures*, 22, (1986), 111 – 119.

Lu, K.; Accorsi, M.; Leonard, J.: Finite element analysis of membrane wrinkling. *International Journal for Numerical Methods in Engineering*, 50, (2001), 1017 – 1038.

Miehe, C.: Entropic thermoelasticity at finite strains. aspects of the formulation and numerical implementation. *Computer Methods in Applied Mechanics and Engineering*, 120, (1995), 243 – 269.

Miller, R. K.; Hedgepeth, J. M.; Weingarten, V. I.; Das, P.; Kahayi, S.: Finite element analysis of partly wrinkled membranes. *Computers & Structures*, 20, (1985), 631 – 639.

Müller, I.; Strehlow, P.: *Rubber and Rubber Balloons*. Springer, Berlin (2004).

Otto, F.; Trostel, R.: *Zugbeanspruchte Konstruktionen*. Ullstein Fachverlag, Frankfurt, Berlin (1962).

Raible, T.: *Concepts for nonlinear orthotropic material modeling with applications to membrane structures*. Institut für Baumechanik und Numerische Mechanik, Universität Hannover (2003).

Roddeman, D.: The wrinkling of thin membranes: Part i – theory. *Journal of Applied Mechanics*, 54, (1987), 884 – 887.

Schoop, H.; Taenzer, L.; Hornig, J.: Wrinkling of nonlinear membranes. *Computational Mechanics*, 29, Number 1, (2002), 68 – 74.

Seokwoo, K.; Seyoung, I.: Finite element analysis of wrinkling membranes. *Journal of Applied Mechanics*, 64, (1997), 263 – 269.

Taenzer, L.: *Strukturdynamische Modellierung und statische Berechnung von Segelkonstruktionen*. Shaker-Verlag, Aachen (1997).

Tietze, P.: *Finite-Elemente Anwendungen eines isotropen, elastisch-plastischen Stoffgesetzes im Dehnungsraum*. VDI-Verlag, Düsseldorf (1986).

Wiedemann, B.: *Modelle für vorgespannte Membranen mit Faltenbildung*. Institut für Statik, TU Braunschweig (2002).

Ziegler, R.; Wagner, W.; Bletzinger, K. U.: *A multisurface concept for the finite – element analysis of wrinkled membranes*. IASS – IACM (2000).

Addresses: Jörg Hornig, Blumenthalstr. 9, D–28209 Bremen
`Joerg.Hornig@airbus.com`
Heinrich Schoop, TU Berlin Institut für Mechanik, Sekr. MS 1 Einsteinufer 5-7, D–10587 Berlin
`HeinrichSchoop@aol.com`
Uwe Herbrich, TU Berlin Institut für Mechanik, Sekr. C 8, Strasse des 17. Juni 135, D–10623 Berlin
`Uwe.Herbrich@TU-Berlin.DE`